
NEUTRAL PARTICLE MOTION AROUND A SCHWARZSCHILD-DE SITTER BLACK HOLE IN $f(\mathcal{R})$ GRAVITY

Devansh Shukla

Sardar Vallabhbhai National Institute of Technology, Surat, India
devanshshukla99@gmail.com

Kamlesh Pathak

Sardar Vallabhbhai National Institute of Technology, Surat, India
knp@phy.svnit.ac.in

ABSTRACT

This article investigates the presence of a static spherically symmetric solution in the metric $f(\mathcal{R})$ gravity. Consequently, we have examined the presence of horizons for the extreme and hyperextreme Schwarzschild-de Sitter solution. Further, we have investigated the orbital motion of a time-like particle around the Schwarzschild-dS solution by forming the constraints for the existence of circular orbits and have subsequently developed an approximation to the innermost stable circular orbit (ISCO).

1 Introduction

Einstein initially proposed the theory of General Relativity in 1915[1, 2]. Now, over a century later, concerns regarding its limitations are increasingly prominent. Although, Einstein's General Relativity has stood observational and experimental scrutiny, it falls short of explaining recent cosmological and astrophysical data such as galactic rotation curves and cosmic inflation.

Recent cosmological evidence, primarily derived from type Ia supernovae explosions, indicates that the universe is indeed undergoing acceleration[3]. However, GR fails to explain this without invoking minuscule cosmological constant or a form of dark energy[4, 5]. The most basic model that which fits the observational data is the concordance or standard Λ Cold Dark Matter(Λ CDM) model with some inflationary scenario, with a field called inflaton[5]. Even so, it is also plagued by various challenges. It neither explains the nature of the inflationary field nor the nature of dark energy or matter. Furthermore, it is plagued by the coincidence problem, horizon problem, and some physicists find the degree of fine-tuning to be disconcerting[6, 7].

Additionally, it is expected that Einstein's theory breaks down at extremely high energy levels near the Planck's scale, where higher order curvature terms dominates and can no longer be neglected[4]. Thus, providing sufficient motivation to study modified gravity theories which can consider those higher order curvature terms, like $f(\mathcal{R})$ theories of gravity.

$f(\mathcal{R})$ theories of gravity is a family of theories, each defined with a different function of the Ricci scalar, \mathcal{R} . These theories arise by a straightforward generalization of the Lagrangian in the Einstein-Hilbert action to become a general function[5] of \mathcal{R} as:

$$S = \frac{1}{2\kappa} \int d^4x \sqrt{-g} f(\mathcal{R}) \quad (1)$$

It was first proposed by Hans Adolf Buchdahl in 1970s and later matured and used by Starobinsky for explaining the cosmic inflation[8]. $f(\mathcal{R})$ theories of gravity are an interesting and relatively simple modification to Einstein's General Relativity[1, 2]. Although, it is relatively straightforward to handle, its action is adequately comprehensive to encompass some fundamental attributes of higher-order gravity.

There exist three versions of $f(\mathcal{R})$ gravity. The first version is defined using the metric formalism[9], the second version is known as Palatini's $f(\mathcal{R})$ gravity[10] and is defined in the Palatini formalism, and the third version is the metric-affine $f(\mathcal{R})$ gravity[11]. The metric-affine $f(\mathcal{R})$ gravity represents the most general and comprehensive form, which can be simplified to metric or Palatini $f(\mathcal{R})$ gravity given specific assumptions.

In this article, we will utilize the metric formalism for $f(\mathcal{R})$ gravity. However, as obvious from previous literatures[12], the equations prove to be a significant challenge for analytical solutions without additional simplifying assumptions. So, we will employ the popular option of using constant scalar curvature(R_0) with Eq. (2).

$$f(R_0) = \partial_r f(R_0) = 0 \quad (2)$$

Further, we will assume a static spherically symmetric metric to obtain the line-element for a Schwarzschild-de Sitter black hole in $f(\mathcal{R})$ gravity. While the general relativity does not always allow for the consideration of circular motion of a test particle, it remains valuable in numerous theoretical investigations such as the study of spacetime geometry, understanding accretion disks, and analyzing geodesic motion. Therefore, we will outline the constraints and solutions pertaining to the horizons of the Schwarzschild-dS black hole[30], as well as the existence of circular orbits such as the marginally stable circular orbit (MSCO) and the inner-most stable circular orbit (ISCO)[13, 14].

The paper is organized as follows. In section 2, we provide a brief explanation of the metric formalism of $f(\mathcal{R})$ gravity and develop the field equations. In section 3, we analyze the ansatz model for the static spherically symmetric solution and examine the metric. Section 4 deals with computing the horizons for near-extreme Schwarzschild-de Sitter blackhole and existence of holes in hyperextreme case. In Section 5, we utilize the line-element obtained in Section 3 to develop an effective potential and develop the conditions for the existence of circular orbits. Later in the section, we develop the marginally stable circular orbits and prove it as the approximation to the innermost stable circular orbits for time like particles in $f(\mathcal{R})$ gravity. Finally, in section 6, we summarize the results.

We use the natural units $c = G = k_B = \hbar = 1$ with the metric convention of $(-, +, +, +)$ throughout the paper.

2 The ansatz model

In order to obtain the ansatz model for $f(\mathcal{R})$ gravity, we attempt to generalize the Einstein-Hilbert action by replacing the ricci scalar \mathcal{R} by an arbitrary function of the scalar curvature $f(\mathcal{R})$. The generalization is real and important and we use it to compute the Einstein-Hilbert action:

The modified Einstein-Hilbert action reads

$$A_g = \frac{1}{2\kappa} \int d^4x \sqrt{-g} f(\mathcal{R}) \quad (3)$$

The total action reads:

$$A = A_g + A_m \quad (4)$$

where A_m represents the matter action. We develop the field equation by varying the action with respect to the metric:

$$\begin{aligned} \frac{\delta A}{\delta g^{\mu\nu}} &= \frac{1}{2\kappa} \int \frac{\delta}{\delta g^{\mu\nu}} \{d^4x \sqrt{-g} f(\mathcal{R})\} + \frac{\delta A_m}{\delta g^{\mu\nu}} \\ \frac{\delta A_g}{\delta g^{\mu\nu}} &= \frac{1}{2\kappa} \int d^4x \left\{ \left(\frac{\delta}{\delta g^{\mu\nu}} \sqrt{-g} \right) f(\mathcal{R}) + \sqrt{-g} f'(\mathcal{R}) \frac{\delta \mathcal{R}}{\delta g^{\mu\nu}} \right\} \end{aligned} \quad (5)$$

where $f'(\mathcal{R}) = \partial_{\mathcal{R}} f(\mathcal{R})$

The variation of the scalar tensor is computed from the definition:

$$\begin{aligned} \frac{\delta \mathcal{R}}{\delta g^{\mu\nu}} &= \frac{\delta}{\delta g^{\mu\nu}} (g^{\mu\nu} \mathcal{R}_{\mu\nu}) \\ \frac{\delta \mathcal{R}}{\delta g^{\mu\nu}} &= \mathcal{R}_{\mu\nu} + g_{\mu\nu} \square - \nabla_\mu \nabla_\nu \end{aligned} \quad (6)$$

where $\square \equiv g^{\alpha\beta} \nabla_\alpha \nabla_\beta$

Using Eq. (6) with Eq. (5), we obtain:

$$\delta A_g = \frac{1}{2\kappa} \int d^4x \left\{ -\frac{1}{2} \sqrt{-g} g_{\mu\nu} \delta g^{\mu\nu} f(\mathcal{R}) + \sqrt{-g} f'(\mathcal{R}) \{ \delta g^{\mu\nu} \mathcal{R}_{\mu\nu} + g_{\mu\nu} \square \delta g^{\mu\nu} - \nabla_\mu \nabla_\nu \delta g^{\mu\nu} \} \right\} \quad (7)$$

$$\delta A_g = \frac{1}{2\kappa} \int d^4x \sqrt{-g} \delta g^{\mu\nu} \left\{ \mathcal{R}_{\mu\nu} f'(\mathcal{R}) - \frac{1}{2} g_{\mu\nu} f(\mathcal{R}) - (\nabla_\mu \nabla_\nu - g_{\mu\nu} \square) f'(\mathcal{R}) \right\} \quad (8)$$

Using Eq. (5) and Eq. (8), the field equations reads:

$$\mathcal{R}_{\mu\nu} f'(\mathcal{R}) - \frac{1}{2} g_{\mu\nu} f(\mathcal{R}) - (\nabla_\mu \nabla_\nu - g_{\mu\nu} \square) f'(\mathcal{R}) = \kappa T_{\mu\nu} \quad (9)$$

$$\text{with } T_{\mu\nu} = \frac{-2}{\sqrt{-g}} \frac{\delta A_m}{\delta g^{\mu\nu}}$$

3 Static spherically symmetric solution

In order to obtain the Schwarzschild's line element, we assume an ansatz solution for the spherically symmetric solution characterised by the radial coordinate with the anomalous red shift $\phi(r)$ [15]:

$$ds^2 = -e^{-2\phi(r)} Z(r) dt^2 + Z^{-1}(r) dr^2 + r^2 d\Omega_k^2 \quad (10)$$

Here $d\Omega_k^2$ is the metric of a constant curvature two-dimensional space, with three different possible topologies namely spherical ($k = 1$), flat ($k = 0$) and hyperbolic ($k = -1$).

$$d\Omega_k^2 = \frac{1}{1 - k\rho^2} d\rho^2 + \rho^2 d\phi^2 \quad (11)$$

Evaluating the Ricci scalar using the metric defined in Eq. (10):

$$\mathcal{R} = \frac{2k + r^2 (-Z''(r)) + Z(r) (2r^2 \phi''(r) - 2r^2 \phi'(r)^2 + 4r\phi'(r) - 2) + rZ'(r) (3r\phi'(r) - 4)}{r^2} \quad (12)$$

where $Z'(r) = \partial_r Z(r)$ and $\phi'(r) = \partial_r \phi(r)$

Adopting a constant scalar curvature $\mathcal{R} = R_0$ and the simplest case of anomalous red-shift where $\phi(r) = \phi$, this implies that $\phi'(r)$ and all further derivatives vanishes, leaving a trivial second-order differential equation Eq. (13):

$$R_0 = \frac{2k - r^2 Z''(r) - 4rZ'(r) - 2Z(r)}{r^2} \quad (13)$$

The solution of Eq. (13) can be expressed as Eq. (14). It is worth noting that the obtained solution bears resemblance to the Nariai solution, which is discussed further in the next section.

$$Z(r) = k + \frac{C_1}{r} + \frac{C_2}{r^2} - \frac{r^2 R_0}{12} \quad (14)$$

Here, anti-de Sitter (AdS) and de Sitter (dS) space are denoted by the appropriate values of k and the scalar curvature R_0 respectively. This article exclusively focuses on the de Sitter treatment, hence, $R_0 > 0$ and $k = 1$.

The solution for our static spherically symmetric line element with reads:

$$ds^2 = - \left(1 + \frac{C_1}{r} + \frac{C_2}{r^2} - \frac{r^2 R_0}{12} \right) dt^2 + \left(1 + \frac{C_1}{r} + \frac{C_2}{r^2} - \frac{r^2 R_0}{12} \right)^{-1} dr^2 + r^2 d\Omega^2 \quad (15)$$

In the upcoming section, we will calculate the value of horizons using the computed line element.

4 Investigation of horizons

By utilizing the static spherically symmetric line element derived in the previous section, we can express g_{tt} as:

$$g_{tt}(r) = - \left(1 + \frac{C_1}{r} + \frac{C_2}{r^2} - \frac{r^2 R_0}{12} \right) \quad (16)$$

The Eq. (16) bears resemblance to the Schwarzschild-dS solution in vanilla general relativity.

The Schwarzschild-de Sitter is the generalization of the Schwarzschild solution with mass parameter m and an arbitrary cosmological constant Λ [16, 30]. The metric for this case was discovered by Kottler[17], Weyl[18] and Trefftz[19] and can be written as:

$$ds^2 = - \left(1 - \frac{2m}{r} - \frac{\Lambda}{3} r^2 \right) dt^2 + \left(1 - \frac{2m}{r} - \frac{\Lambda}{3} r^2 \right)^{-1} dr^2 + r^2 (d\theta^2 + \sin^2 \theta d\phi^2) \quad (17)$$

This solution reduces to Schwarzschild metric when $\Lambda = 0$ and to de Sitter or anti-de Sitter metric in their spherically symmetric forms when $m = 0$ [30].

By comparing the g_{tt} component in our SSS line-element with that of the Schwarzschild-dS solution, we can assume that C_2 vanishes. Although, eliminating C_2 will reduce the number of independent variables, but it will significantly simplify our calculations from a quartic equation to a cubic equation. Furthermore, it is demonstrated in multiple articles that $C_2 = Q$ and corresponds to Reissner-Nordström solution as charge Q [12, 20].

Additionally, given that the theory must conform to standard general relativity when there is no curvature (R_0), we can infer that $C_1 = -2m$ and $\frac{R_0}{4} = \Lambda$ [12]

The $g_{tt}(r)$ becomes:

$$g_{tt}(r) = \frac{1}{12r} (R_0 r^3 - 12r + 24m) \quad (18)$$

Our primary focus is on understanding the characteristics of g_{tt} . Therefore, we will exclusively concentrate on the cubic polynomial at this moment:

$$R_0 r^3 - 12r + 24m \quad (19)$$

The discriminant for the cubic polynomial in Eq. (19) can be expressed as:

$$\Delta_3 = 432R_0 (16 - 9(4m^2)R_0) \quad (20)$$

Trivially, it can be noted that for $\Delta_3 > 0$: there are three distinct real roots, whereas for $\Delta_3 < 0$: there is one real root and two complex conjugate roots and for $\Delta_3 = 0$: all roots are real but two are repeated roots.

In order to achieve a positive Δ_3 , the following condition must be true:

$$R_0 (4 - 9m^2 R_0) > 0 \quad (21)$$

Therefore, for a deSitter spacetime, the relation between C_1 and R_0 to obtain a positive discriminant is given as:

$$\boxed{0 < \frac{9m^2}{4} R_0 < 1} \quad (22)$$

Following the constraint in the above equation, we can compute the roots for the Eq. (19) using the trigonometric method for solving depressed cubic equations, as originally derived by François Viète[21].

$$\begin{aligned} r_1 &= 4\sqrt{\frac{1}{R_0}} \cos\left(\frac{1}{3} \arccos\left(-\frac{3}{2}m\sqrt{R_0}\right)\right) \\ r_2 &= -4\sqrt{\frac{1}{R_0}} \sin\left(\frac{\pi}{6} - \frac{1}{3} \arccos\left(-\frac{3}{2}m\sqrt{R_0}\right)\right) \\ r_3 &= -4\sqrt{\frac{1}{R_0}} \sin\left(\frac{1}{3} \arccos\left(-\frac{3}{2}m\sqrt{R_0}\right) + \frac{\pi}{6}\right) \end{aligned} \quad (23)$$

Furthermore, since Eq. (19) is a depressed cubic polynomial with no 2^{st} order term, the sum of its roots must be zero. Consequently, the third root will be negative and equal to the sum of the other two roots.

In Fig. (1), we are assuming the value of mass to be unity for simplicity. However, this assumption does not result in any loss of degrees of freedom due to the constraint described in Eq. (22).

Upon analyzing Fig. (1), it is evident that initially the value of r_1 is infinitely large while the value of r_2 is 2. As both approach the extremum limit in deSitter space-time, they both collapse to a shared value of 3. This is consistent with the concept that r_1 represents the cosmological horizon and r_2 represents the Schwarzschild black hole horizon.

There are no real horizons distances in the hyperextreme case $\left(\frac{9R_0 m^2}{4} > 1\right)$ so there are no blackholes just naked singularity without horizons[22, 30].

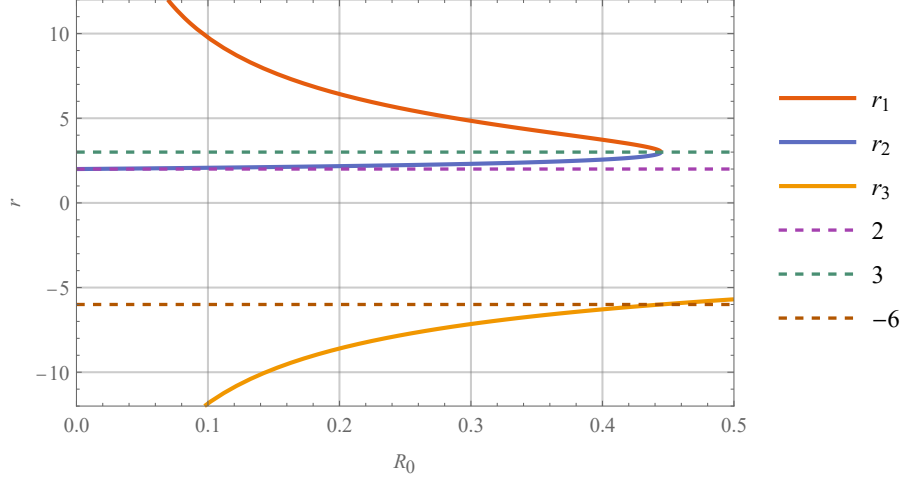


Figure 1: Plot for r vs R_0 assuming unit mass ($m=1$) and deSitter space-time

5 Circular orbit solution

We will now work towards computing the innermost stable circular orbit for our static spherically symmetric solution.

$$Z(r) = 1 + \frac{C_1}{r} + \frac{C_2}{r^2} - \frac{r^2 R_0}{12} \quad (24)$$

Let us assume a test particle of a non-negative μ in the equatorial frame ($\theta = \pi/2$). The line element reads:

$$ds^2 = g_{\alpha\beta} dx^\alpha dx^\beta = -Z(r) dt^2 + \frac{1}{Z(r)} dr^2 + r^2 d\phi^2 = \epsilon \quad (25)$$

where $\epsilon = -1, 0, 1$ for timelike, null-like and spacelike trajectories respectively.

The lagrangian of a free particle in a potential-less spacetime reads:

$$\mathcal{L} = \mu \sqrt{g_{\alpha\beta} \dot{x}^\alpha \dot{x}^\beta} \quad (26)$$

Considering our lagrangian is independent of t and ϕ , the first integrals of motion obtained using the Euler-Lagrange equation reads:

$$\mu Z(r) \dot{t} = E; \quad \mu r^2 \dot{\phi} = L \quad (27)$$

where E and L represent the energy and angular momentum of the test particle respectively.

Substituting Eq. (27) into Eq. (25):

$$-\frac{E^2}{\mu^2 Z(r)} + \frac{\dot{r}^2}{Z(r)} + \frac{L^2}{\mu^2 r^2} = \epsilon \quad (28)$$

$$\dot{r}^2 + V_{\text{eff}}^2 = \frac{E^2}{\mu^2} \quad (29)$$

with the effective potential represented by:

$$V_{\text{eff}} = \sqrt{\left(\frac{L^2}{\mu^2 r^2} - \epsilon \right) Z(r)} \quad (30)$$

The circular orbits are determined by the condition that $\dot{r} = 0$. These circular orbits sit at critical points of the effective potential V_{eff} , or simply $V'_{\text{eff}}(r_o) = 0$ [23, 24]. The extremum values of V'_{eff} determines both the stable and unstable circular orbits for the test particle. For the orbit to achieve classical stability, it is necessary that r_o satisfies $V''_{\text{eff}}(r_o) > 0$ [24, 25].

The notion of innermost stable circular orbits (ISCO) r_{isco} corresponds to the marginally stable circular orbits[23, 26] which satisfies both: $V'_{\text{eff}}(r_{\text{isco}}) = V''_{\text{eff}}(r_{\text{isco}}) = 0$

Solving for $\partial_r V_{\text{eff}} = 0$, we obtain the value of the angular momentum and energy as:

$$\frac{L^2}{r^2 \mu^2} = \frac{\epsilon (6C_1 r + 12C_2 + r^4 R_0)}{6(3C_1 r + 4C_2 + 2r^2)} \quad (31)$$

$$\frac{E^2}{\mu^2} = -\frac{\epsilon (12C_1 r + 12C_2 - r^4 R_0 + 12r^2)^2}{72r^2 (3C_1 r + 4C_2 + 2r^2)} \quad (32)$$

By choosing $\epsilon = -1$, we restrict our analysis to exclusively timelike orbits. To streamline the calculation process, we will employ the assumption derived from the previous section: $C_1 = -2m$ and $C_2 = 0$

In this case, the corresponding angular momentum and potential can be expressed as:

$$\frac{L^2}{\mu^2} = \frac{r^2}{12} \left(\frac{r^3 R_0 - 12m}{3m - r} \right) \quad (33)$$

$$\frac{E^2}{\mu^2} = -\frac{(24m + r^3 R_0 - 12r)^2}{144r(3m - r)} \quad (34)$$

Analyzing Eq. (33) indicates that in order for L^2/μ^2 to have a positive value when r exceeds $3m$, the expression $r^3 R_0 - 12m$ must be negative. Therefore, we obtain the following constraint for the radial parameter of a circular orbit:

$$3m < r < \left(\frac{12m}{R_0} \right)^{1/3} \quad (35)$$

The inverse scenario when $r < 3m$, the expression $(r^3 R_0 - 12m)$ must be positive. By substituting the max value of scalar curvature permitted by constraint Eq. (22), it becomes evident that this scenario is not possible.

Now, in order to compute the innermost stable circular orbit we again extremise the potential V_{eff} , given by Eq. (30), and solve for r :

$$(r^3 R_0 - 12r + 24m) (r^3 R_0 (4r - 15m) + 12m(6m - r)) = 0 \quad (36)$$

The first part of Eq. (36) is simply the polynomial we solved in the earlier section and obtained the blackhole and cosmological horizons value. In this section, we will focus on the second part of the equation, the fourth order polynomial for finding the circular orbits:

$$(r^3 R_0 (4r - 15m) + 12m(6m - r)) = 0 \quad (37)$$

In order to ascertain the nature of roots, we first compute the discriminant for the fourth order polynomial Eq. (37) as:

$$\Delta_4 = -8957952m^4 R_0^2 (9m^2 R_0 - 4) (5625m^2 R_0 - 16) \quad (38)$$

Trivially, it can be noted that for: $\Delta_4 > 0$: there exists four real roots or 2 pairs of conjugated complex roots, $\Delta_4 = 0$: there exists a minimum 2 complex/real roots are repeated, $\Delta_4 < 0$: there exists a pair of conjugated complex roots and two real roots, all of these are distinct.

So, in hopes of obtaining real and distinct roots, assuming $m > 0$ and $R_0 > 0$, we see that the discriminant is negative for $(9m^2 R_0 - 4) < 0$ and $(5625m^2 R_0 - 16) < 0$, or simply:

$$0 < m^2 R_0 < \frac{16}{5625} \quad (39)$$

Now, by solving the quartic equation given in Eq. (37) using Mathematica[27], we find the real roots as:

$$\begin{aligned} r_{o1} &= \frac{15m}{16} + \frac{1}{16} \left[9m^2 \left(96 \cdot 6^{1/3} \Xi^{-1} + 25 \right) + \frac{16 \cdot 6^{2/3} \Xi}{R_0} \right]^{1/2} \\ &\quad - \frac{1}{16} \left[450m^2 - \frac{16 \cdot 6^{2/3} \Xi}{R_0} - 864 \cdot 6^{1/3} m^2 \Xi^{-1} + \frac{6m (1125m^2 R_0 + 512)}{R_0 \left[9m^2 (96 \cdot 6^{1/3} \Xi^{-1} + 25) + \frac{16 \cdot 6^{2/3} \Xi}{R_0} \right]^{1/2}} \right]^{1/2} \\ r_{o2} &= \frac{15m}{16} + \frac{1}{16} \left[9m^2 \left(96 \cdot 6^{1/3} \Xi^{-1} + 25 \right) + \frac{16 \cdot 6^{2/3} \Xi}{R_0} \right]^{1/2} \\ &\quad + \frac{1}{16} \left[450m^2 - \frac{16 \cdot 6^{2/3} \Xi}{R_0} - 864 \cdot 6^{1/3} m^2 \Xi^{-1} + \frac{6m (1125m^2 R_0 + 512)}{R_0 \left[9m^2 (96 \cdot 6^{1/3} \Xi^{-1} + 25) + \frac{16 \cdot 6^{2/3} \Xi}{R_0} \right]^{1/2}} \right]^{1/2} \end{aligned} \quad (40)$$

where $\Xi = \left[m^2 R_0 \left(225m^2 R_0 + \sqrt{50625m^4 R_0^2 - 22644m^2 R_0 + 64} + 8 \right) \right]^{1/3}$

The second derivative of the effective potential, $V_{\text{eff}}''(r)$ can be represented as Eq. (41). In order for the circular orbit solutions to be stable, it is necessary that the second derivative of the effective potential must be positive, $V_{\text{eff}}'' > 0$. However, the analytical verification for $V_{\text{eff}}''(r_{\text{msco}}) > 0$ is difficult; instead, we can easily demonstrate it through Fig. (2)

$$V_{\text{eff}}''(r) = \frac{(24m + r^3 R_0 - 12r) (12m (54m^2 - 39mr + 4r^2) + r^3 R_0 (135m^2 - 60mr + 8r^2))}{48(r(r - 3m))^{5/2} |R_0 r^3 - 12r + 24m|} \quad (41)$$

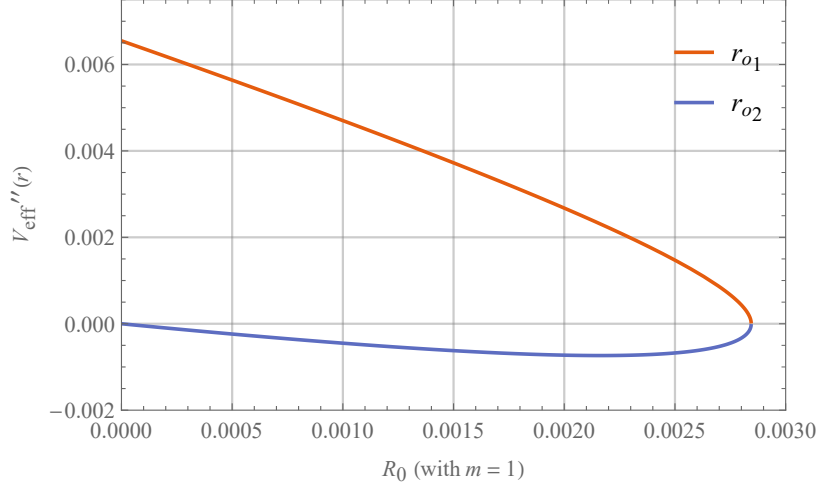


Figure 2: Plot for V_{eff}'' vs R_0 for both roots r_{o1} and r_{o2}

As evident from Fig. (2), r_{o1} represents a stable circular orbit whereas r_{o2} is unstable and would inevitably plunge into the black hole.

Therefore, the marginally stable circular orbit is:

$$r_{\text{msco}} = \frac{15m}{16} + \frac{1}{16} \left[9m^2 \left(96 \cdot 6^{1/3} \Xi^{-1} + 25 \right) + \frac{16 \cdot 6^{2/3} \Xi}{R_0} \right]^{1/2} - \frac{1}{16} \left[450m^2 - \frac{16 \cdot 6^{2/3} \Xi}{R_0} - 864 \cdot 6^{1/3} m^2 \Xi^{-1} + \frac{6m (1125m^2 R_0 + 512)}{R_0 \left[9m^2 (96 \cdot 6^{1/3} \Xi^{-1} + 25) + \frac{16 \cdot 6^{2/3} \Xi}{R_0} \right]^{1/2}} \right]^{1/2} \quad (42)$$

Furthermore, under $R_0 \rightarrow 0$, the modified theory has to converge back to standard general relativity. Applying this limit to r_{msco} with $m = 1$ yields a value of 6.00016, which is an extremely close approximation to Einstein's relativity ISCO of 6.00. Additionally, as shown in Fig. (2), the V_{eff}'' does not vanish but is a good approximation to zero. As a result, r_{msco} , the solution we calculated, is a reasonable approximation to r_{isco} .

$$r_{\text{isco}} \approx \frac{15m}{16} + \frac{1}{16} \left[9m^2 \left(96 \cdot 6^{1/3} \Xi^{-1} + 25 \right) + \frac{16 \cdot 6^{2/3} \Xi}{R_0} \right]^{1/2} - \frac{1}{16} \left[450m^2 - \frac{16 \cdot 6^{2/3} \Xi}{R_0} - 864 \cdot 6^{1/3} m^2 \Xi^{-1} + \frac{6m (1125m^2 R_0 + 512)}{R_0 \left[9m^2 (96 \cdot 6^{1/3} \Xi^{-1} + 25) + \frac{16 \cdot 6^{2/3} \Xi}{R_0} \right]^{1/2}} \right]^{1/2} \quad (43)$$

Fig. (3a) displays the graph of our approximated solution for the Innermost Stable Circular Orbit (ISCO) as a function of R_0 whereas Fig. (3b) displays ISCO as a function of m considering $R_0 \rightarrow 0$, assuming unit mass ($m = 1$).

It is evident from Fig. (3) that the approximated solution for ISCO behaves quadratically with R_0 for $m \rightarrow 1$ and linearly with m for $R_0 \rightarrow 0$. It is important to remember that the limits determined by Eq. (39) constrain the ISCO solution.

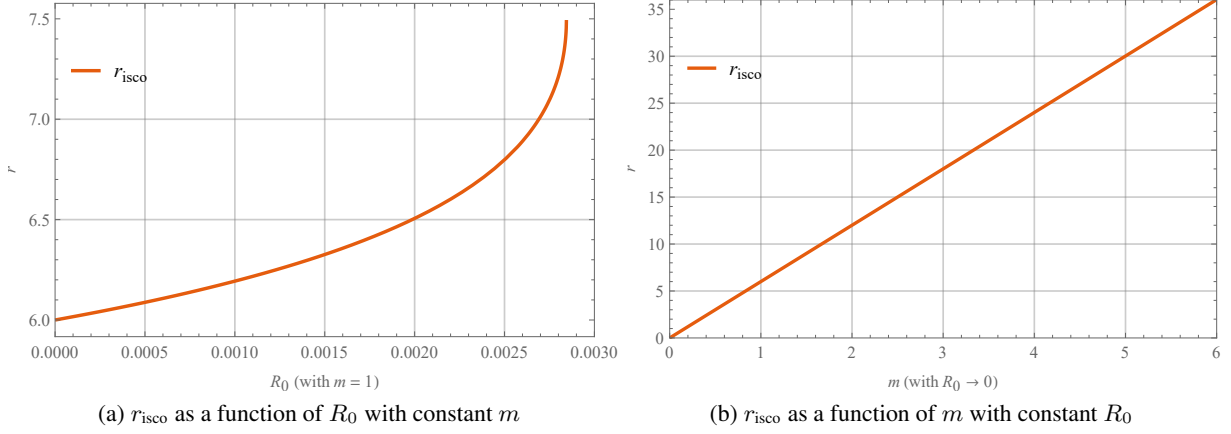


Figure 3: Approximated ISCO solution as a function of R_0 with constant m and vice-versa

Through Fig. (4), we can illustrate the nature of different properties we computed earlier like, angular momentum Eq. (33), effective potential Eq. (30) and its derivatives as a function of our approximated ISCO solution.

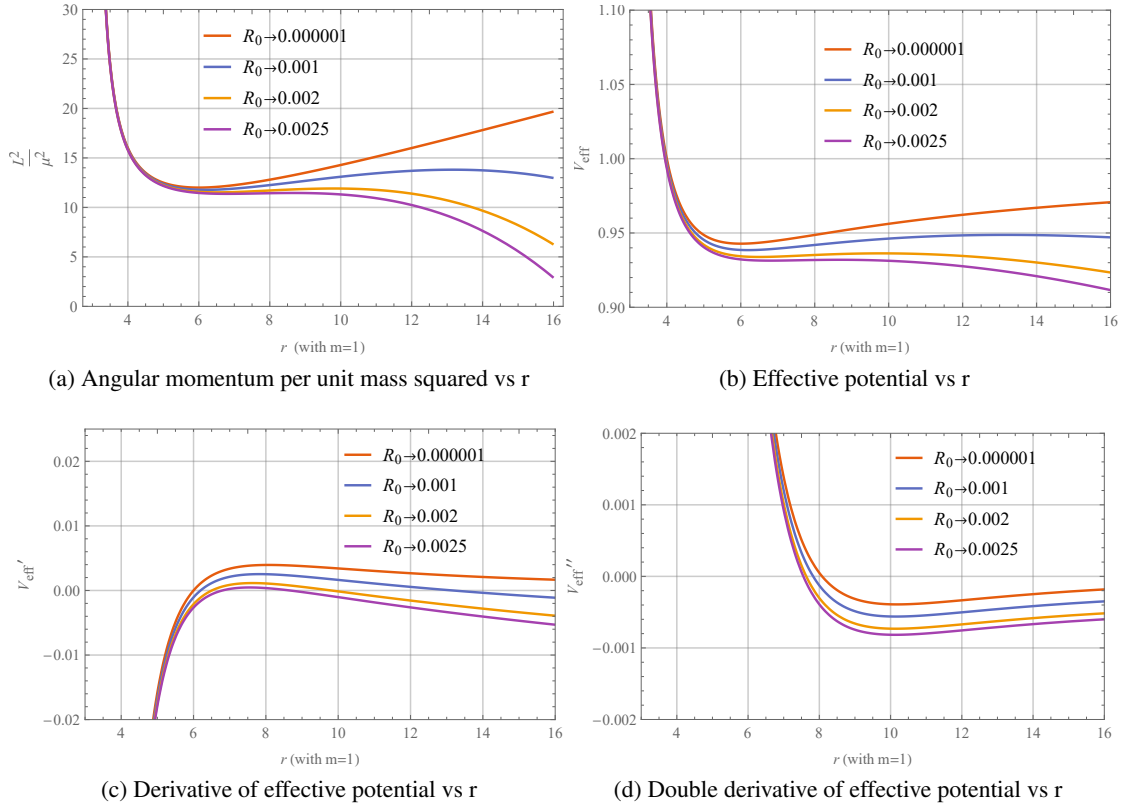


Figure 4: Plot of (a) $\frac{L^2}{\mu^2}$, (b) $V_{\text{eff}}(r)$, (c) $V'_{\text{eff}}(r)$, (d) $V''_{\text{eff}}(r)$ as a function of r for $R_0 = 10^{-6}, 0.001, 0.002, 0.0025$ with $m = 1$

6 Conclusion

In this article, we have developed a solution for a static spherically symmetric solution under the metric formalism of $f(\mathcal{R})$ gravity. Subsequently, we employed the aforementioned solution and compared it with the Schwarzschild-de Sitter solution in order to determine the values of the constants C_1 and C_2 as $-2m$ and 0 , respectively. The selection of these particular values was essential for obtaining the solutions for black hole and cosmological horizons for our near-extreme Schwarzschild-dS case. We confirmed that these solutions converge to Einstein's standard general relativity when the limits of $m \rightarrow 1$ and $R_0 \rightarrow 0$ are applied. Additionally, using these constants we computed the existence constraints for extreme and hyperextreme Schwarzschild-de Sitter blackholes.

It is apparent to observe that our static spherically symmetric line-element Eq. (15) reduces to Schwarzschild's line element for $r \rightarrow 0$ or for near-zero scalar curvature. On the other hand, it becomes the de Sitter line element when $r \rightarrow \infty$ or there's curvature present.

In section 5, we calculated the solutions for circular orbits and demonstrated their stability. Subsequently, we were able to approximate these marginally stable circular orbit as the innermost stable circular orbit. It is evident from Fig. (3) that the approximated ISCO solution is quadratic with R_0 with m being a constant and linear with m with R_0 being a constant. In addition, we were able to compute the nature of angular momentum, effective potential and its derivatives using the approximated ISCO solution in Fig. (4).

References

- [1] Albert Einstein. The Field Equations of Gravitation. *Sitzungsber. Preuss. Akad. Wiss. Berlin (Math. Phys.)*, 1915:844–847, 1915.
- [2] Albert Einstein. The foundation of the general theory of relativity. *Annalen Phys.*, 49(7):769–822, 1916.
- [3] Adam G. Riess, Alexei V. Filippenko, Peter Challis, Alejandro Clocchiatti, Alan Diercks, Peter M. Garnavich, Ron L. Gilliland, Craig J. Hogan, Saurabh Jha, Robert P. Kirshner, B. Leibundgut, M. M. Phillips, David Reiss, Brian P. Schmidt, Robert A. Schommer, R. Chris Smith, J. Spyromilio, Christopher Stubbs, Nicholas B. Suntzeff, and John Tonry. Observational evidence from supernovae for an accelerating universe and a cosmological constant. *The Astronomical Journal*, 116(3):1009–1038, September 1998.
- [4] C. Charmousis. *Higher Order Gravity Theories and Their Black Hole Solutions*, pages 299–346. Springer Berlin Heidelberg, Berlin, Heidelberg, 2009.
- [5] Thomas P. Sotiriou and Valerio Faraoni. $f(r)$ theories of gravity. *Rev. Mod. Phys.*, 82:451–497, Mar 2010.
- [6] Sean M. Carroll. Lecture notes on general relativity, 1997.
- [7] L. Perivolaropoulos and F. Skara. Challenges for λ -cdm: An update. *New Astronomy Reviews*, 95:101659, 2022.
- [8] A.A. Starobinsky. A new type of isotropic cosmological models without singularity. *Physics Letters B*, 91(1):99–102, 1980.
- [9] Shin'ichi Nojiri and Sergei D. Odintsov. Modified $f(r)$ gravity consistent with realistic cosmology: From a matter dominated epoch to a dark energy universe. *Phys. Rev. D*, 74:086005, Oct 2006.
- [10] Salvatore Capozziello and Mauro Francaviglia. Extended theories of gravity and their cosmological and astrophysical applications. *General Relativity and Gravitation*, 40(2-3):357–420, dec 2007.
- [11] Thomas P. Sotiriou and Stefano Liberati. Metric-affine $f(r)$ theories of gravity. *Annals of Physics*, 322(4):935–966, 2007.
- [12] A. de la Cruz-Dombriz, A. Dobado, and A. L. Maroto. Black holes in $f(r)$ theories. *Phys. Rev. D*, 80:124011, Dec 2009.
- [13] Don N. Page and Kip S. Thorne. Disk-accretion onto a black hole. time-averaged structure of accretion disk. *The Astrophysical Journal*, 191:499–506, July 1974.
- [14] Robert M Wald. *General relativity*. University of Chicago press, 2010.
- [15] Marco Calzà, Massimiliano Rinaldi, and Lorenzo Sebastiani. A special class of solutions in $f(r)$ -gravity. *The European Physical Journal C*, 78(3), mar 2018.
- [16] J. Podolsky. The structure of the extreme schwarzschild-de sitter space-time. *General Relativity and Gravitation*, 31(11):1703–1725, nov 1999.
- [17] Friedrich Kottler. Über die physikalischen grundlagen der einsteinschen gravitationstheorie. *Annalen der Physik*, 361(14):401–462, 1918.

- [18] Hermann Weyl. Über die statischen kugelsymmetrischen lösungen von einsteins “kosmologischen” gravitationsgleichungen. *Physikalische Zeitschrift*, 20:31–34, 1919b.
- [19] E Trefftz. Das statische gravitationsfeld zweier massenpunkte in der einsteinschen theorie. *Mathematische Annalen*, 86:317–326, 1922.
- [20] V. K. Oikonomou. A note on schwarzschild-de sitter black holes in mimetic $f(r)$ gravity. *International Journal of Modern Physics D*, 25(07):1650078, 2016.
- [21] R. W. D. Nickalls. Viète, descartes and the cubic equation. *The Mathematical Gazette*, 90(518):203–208, 2006.
- [22] K. H. Geyer. Geometrie der raum-zeit der maßbestimmung von kottler, weyl und trefftz. *Astronomische Nachrichten*, 301(3):135–149, 1980.
- [23] R. J. Howes. Existence and stability of circular orbits in a Schwarzschild field with nonvanishing cosmological constant. *Australian Journal of Physics*, 32:293–294, jan 1979.
- [24] David Berenstein, Ziyi Li, and Joan Simón. Iscos in ads/cft. *Classical and Quantum Gravity*, 38(4):045009, dec 2020.
- [25] Ibrar Hussain and Sajid Ali. Marginally stable circular orbits in the schwarzschild black hole surrounded by quintessence matter. *The European Physical Journal Plus*, 131(8), August 2016.
- [26] Sheref Nasereldin and Kayll Lake. Boundary orbits: 1 static spacetimes. 2019.
- [27] Wolfram Research, Inc. Mathematica, Version 14.0. Champaign, IL, 2024.
- [28] Lei Qian, Xue-Bing Wu, and Li-Xin Li. The marginally stable circular orbit of the fluid disk around a black hole. 2016.
- [29] Yong Song. The evolutions of the innermost stable circular orbits in dynamical spacetimes. *Eur. Phys. J. C*, 81(10):875, 2021.
- [30] Jerry B. Griffiths and Jiří Podolský. *Exact Space-Times in Einstein’s General Relativity*. Cambridge Monographs on Mathematical Physics. Cambridge University Press, 2009.
- [31] Paul I. Jefremov, Oleg Yu. Tsupko, and Gennady S. Bisnovaty-Kogan. Innermost stable circular orbits of spinning test particles in schwarzschild and kerr space-times. *Phys. Rev. D*, 91:124030, Jun 2015.
- [32] Zdeněk Stuchlík and Petr Slaný. Equatorial circular orbits in the kerr-de sitter spacetimes. *Physical Review D*, 69(6), mar 2004.